Materials Research, Vol. 6, No. 4, 577-581, 2003.

Characterization of $Bi_4Ge_3O_{12}$ Single Crystal by Impedance Spectroscopy

Zélia Soares Macedo[a]*, *André Luiz Martinez*[b], *Antonio Carlos Hernandes*[b]*

[a]*Departamento de Física, Universidade Federal de Sergipe*
C.P. 353, 49100-000 São Cristovão - SE, Brazil
[b]*Instituto de Física de São Carlos, Universidade de São Paulo*
C.P. 369, 13560-970 São Carlos - SP, Brazil

Received: February 10, 2003; Revised: September 8, 2003

$Bi_4Ge_3O_{12}$ (bismuth germanate – BGO) single crystals were produced by the Czochralski technique and their electrical and dielectric properties were investigated by impedance spectroscopy. The isothermal ac measurements were performed for temperatures from room temperature up to 750 °C, but only the data taken above 500 °C presented a complete semicircle in the complex impedance diagrams. Experimental data were fitted to a parallel RC equivalent circuit, and the electrical conductivity was obtained from the resistivity values. Conductivity values from 5.4×10^{-9} to 4.3×10^{-7} S/cm were found in the temperature range of 500 to 750 °C. This electrical conductivity is thermally activated, following the Arrhenius law with an apparent activation energy of (1.41 ± 0.04) eV. The dielectric properties of BGO single crystal were also studied for the same temperature interval. Permittivity values of 20 ± 2 for frequencies higher than 10^3 Hz and a low-frequency dispersion were observed. Both electric and dielectric behavior of BGO are typical of systems in which the conduction mechanism dominates the dielectric response.

Keywords: *bismuth germanate, impedance spectroscopy*

1. Introduction

Bismuth germanate ($Bi_4Ge_3O_{12}$ – BGO), which has a cubic crystalline structure known as eulitine, has been demanded a great deal of interest due to its electro-optic, electro-mechanical and scintillator properties[1-3]. In particular, the use of BGO single crystals in electromagnetic measurements presents many advantages, since it possesses small temperature-dependence of electro-optic effect, high electrical resistivity, no optical activity, no natural birefringence and no pyroelectric effects[2,4]. The use of bismuth germanate as optical fiber sensor for simultaneous measurement of current and voltage was considered recently[5] and it was successfully tested for ac currents from 0.05 to 10 A and voltages from 1 to 235 V.

The literature presents several papers about the BGO crystal structure, scintillation, refractive index, absorption and luminescence over varied wavelengths and conditions. Dielectric permittivity of $Bi_4Ge_3O_{12}$ was reported by Link *et al.*[6] only at 10^3 Hz, in the temperature range from 6 to 325 K, and to our knowledge there is no report on the conductive behaviour of this crystal. The aim of this paper is to present data about the electrical and dielectric parameters of BGO single crystals determined by ac measurements for frequencies between 10^2 and 10^6 Hz, in the temperature interval of 500 to 700 °C. This knowledge would provide a better understanding of the defect structure of this material and it would be an advance in the optimization of their properties.

2. Experimental

BGO single crystals were grown by the Czochralski technique from high temperature stoichiometric compositions, using high purity cylindrical platinum crucibles of 50 cm^3 in volume. BGO seeds oriented along the [0 0 1] direction were held in a pure platinum seed holder and used to initiate the crystal growth. The runs were carried out in room atmosphere and the growing temperature was 1120 °C. The pulling and rotation rates were 0.2 mm/h and 14 rpm, respectively. Transparent single crystals without inclusions were produced with typical sizes of 10 mm in radius and 20 mm in height.

For the impedance spectroscopy measurements, the crystal was cut in slices of $4 \times 4 \times 1$ mm^3 and polished with

*e-mail: zmacedo@fisica.ufs.br, hernandes@if.sc.usp.br
Trabalho apresentado no V Encontro da Sociedade Brasileira de Crescimento de Cristais, Guarujá - SP, 2002.

alumina powder. The samples were cleaned with acetone in ultrasonic bath for 15 min and dried at 100 °C. Electric contact was made by applying Pt paste on the (110) faces of the samples and firing it at 700 °C for 30 min. The measurements were made in the frequency range from 100 Hz to 1 MHz, with an applied potential of 500 mV, using a Solartron 1260 Impedance Analyzer controlled by a personal computer. Isothermal ac measurements were taken from room temperature up to 750 °C. The measured values of impedance $Z^* = Z' + iZ''$ were analyzed using the software Zview[7], adopting equivalent circuits to simulate the immitance spectra and complex diagrams.

3. Results and Discussion

3.1. Electrical Characterization

Figure 1 shows the complex impedance diagrams for measurements acquired at 600, 650, 700 and 750 °C. These complex plots form semicircular arcs, and each experimental point corresponds to a frequency value. The semicircle diameter expresses the electrical resistivity of the sample at the specified temperature and the maximum value corresponds to the relaxation frequency $\omega = 1/RC$. As the impedance measurements performed for BGO below 500 °C did not present a complete semicircle, they were not considered in this study. The diagrams show only the contribution in the high frequency region. No other relaxation mechanism, such as the electrode effect and ionic species diffusion, was identified for the analyzed frequency range[8].

The equivalent circuit adopted to simulate the experimental data consisted in a simple parallel RC. The fitting is exemplified in Fig. 2, which shows the experimental data taken at 750 °C, as well as the simulated curve and the equivalent circuit employed. Good agreement between the experimental and theoretical curves was observed. The electrical properties of $Bi_4Ge_3O_{12}$ crystal can thus be associated with a simple RC equivalent circuit.

The existence of a single relaxation mechanism was corroborated by the plots of the imaginary and real parts of Z^* as functions of the frequency, as seen in Fig. 3. In these plots, shown for T = 750 °C, it was observed only one maximum value of Z'' accompanied by an inflexion point in the Z' curve at the relaxation frequency $f_0 = 1/2\pi RC$. For this temperature $f_0 = 40$ kHz, corresponding to the maximum in the semicircle of the Fig. 2.

Figure 4 shows the electrical conductivity curves of BGO as a function of the signal frequency. The values of σ' were derived from the impedance data using the relation:

$$\sigma' = Z'/(Z'^2 + Z''^2) \quad (1)$$

BGO electrical conductivity presented a frequency independent part at low frequencies followed by a part in which it obeys approximately the universal power law $\sigma'(f) \propto \omega^n$, where $0 < n < 1$ [9,10]. The conductivity value at the plateau (σ'_p) is interpreted as the dc conductivity[11,12].

The behavior of the electrical conductivity with fre-

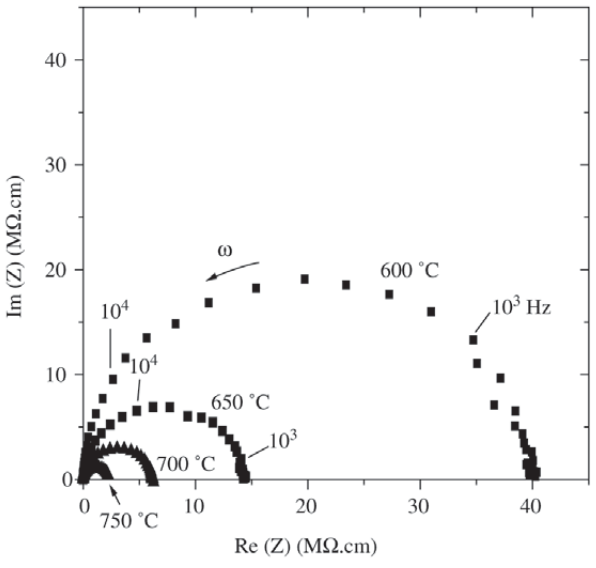

Figure 1. Complex impedance diagrams of $Bi_4Ge_3O_{12}$ single crystal, taken isothermally at 600, 650, 700 and 750 °C. The numbers indicate the signal frequency.

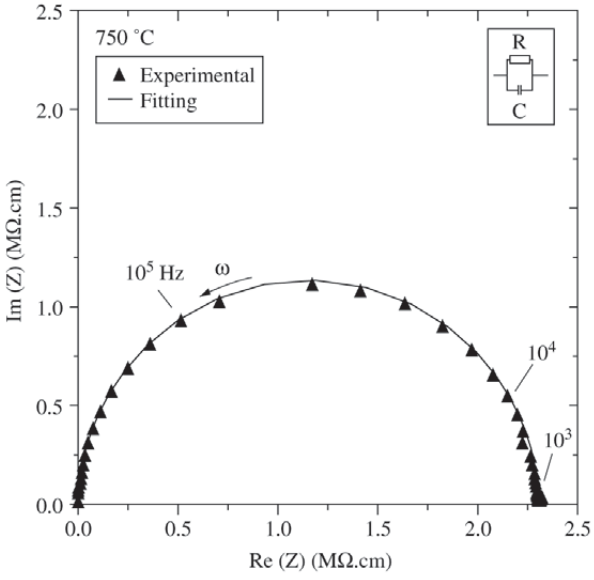

Figure 2. Complex impedance diagrams of $Bi_4Ge_3O_{12}$ taken at 750 °C, fitted to an equivalent RC parallel circuit. The numbers indicate the signal frequency.

quency agrees with that predicted for conduction mechanisms over a random distribution of energy barriers in a disordered solid[12]. For dc conduction the largest energy barriers are overcome, while lower barriers are involved for ac conduction since only a limited distance has to be traveled. At high ac frequencies, the electrical conductivity is increased by the hopping of the charge carrier backward and forward at places with high jump probability. This enhancement in the electrical conductivity continues as long as the frequency of the applied field is lower than the maximum jump frequency in the solid[12]. In $Bi_4Ge_3O_{12}$ structure, the Ge^{4+} possesses a tetrahedra of coordination quite regular, with ions O^{2-} at a distance of 1.740 Å, but the ion Bi^{3+} is coordinated by three ions O^{2-} at 2.160 Å and three ions O^{2-} at 2.605 Å, in a very deformed octaedra[13]. This disorder in BGO structure could account for a distribution of energy barriers for the conduction process, reflected in the dispersion of electrical conductivity values at high frequencies.

The plots in Fig. 4 allow us to evaluate the electrical conductivity σ'_p in the frequency independent interval. These values were taken at the fixed frequency f = 10^3 Hz and used to calculate the apparent activation energy of the process. Additionally, the ac conductivity (σ'_{ac}) of BGO was determined from the complex impedance diagrams, in which the semicircle diameter stands for the resistivity $\rho = 1/\sigma'_{ac}$ of the system. From our results, it was verified that both σ'_p and σ'_{ac} were thermally activated according to the Arrhenius law (see Fig. 5):

$$\sigma' = \sigma_0 \exp(-E_a/kT) \qquad (2)$$

where σ_0 is a pre-exponential factor and E_a, k and T represent the apparent activation energy for conduction process, Boltzmann' constant and the absolute temperature, respectively.

The experimental data shown in Fig. 5 were fitted to Eq. 2 and the apparent activation energy E_a = (1.41 ± 0.04) eV was deduced from the slope of the calculated curve. This energy was the same for both sets of σ'_p and σ'_{ac} values, indicating that the ac conductivity in BGO is dominated by a slow, long-range mechanism.

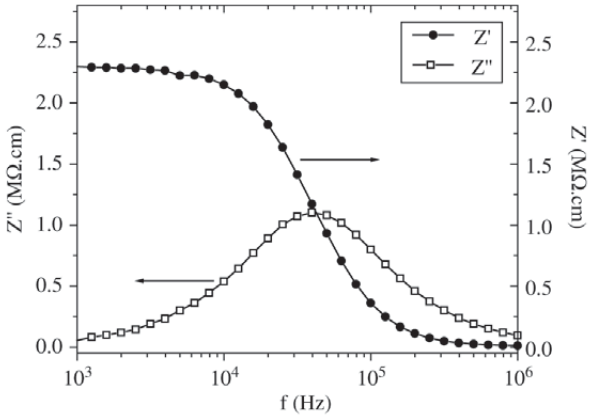

Figure 3. Plots of the imaginary and real parts of Z* as functions of the frequency. The maximum value of Z'' and the inflexion point in the Z' curve are observed at the relaxation frequency $f_0 = 1/2\pi RC$.

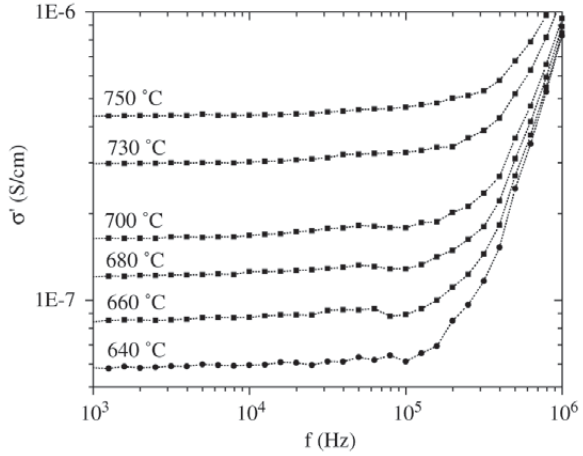

Figure 4. Conductivity σ' of BGO single crystal. The plateau at low frequencies accompanied by the dispersion at high frequencies is generally related to hopping processes in disordered solids[12].

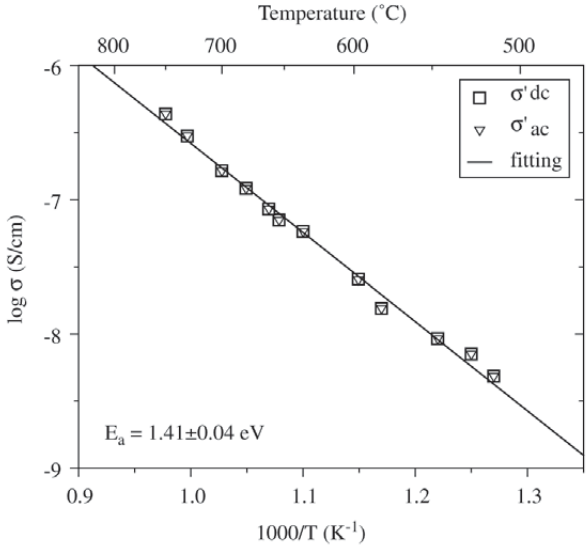

Figure 5. Arrhenius plots for dc and ac conductivities in BGO (σ'_{dc} and σ'_{ac}, respectively). The apparent activation energy indicated in the graphic was deduced from the slope of the linear regression of the data.

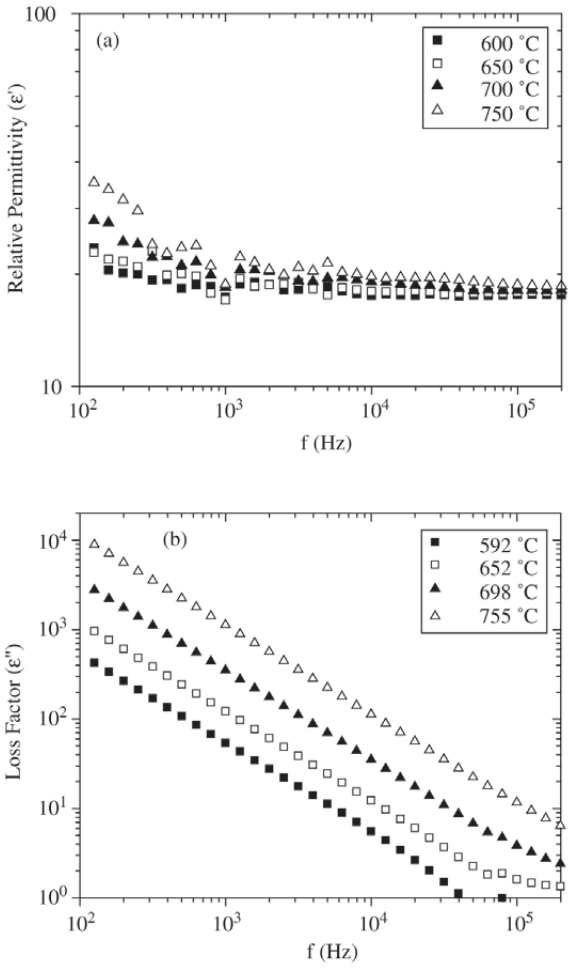

Figure 6. (a) Real part of permittivity ε'; (b) imaginary part of permittivity ε'' as a function of frequency at several temperatures for $Bi_4Ge_3O_{12}$ single crystals.

Among the possible defects in the BGO structure, the most probable one is ion substitution[14], either in the Bi^{3+} or Ge^{4+} sites. Considering that the grouping $(GeO_4)^{4-}$ is very stable the charge compensation, if needed, can be supplied either by the removal of some Bi^{3+} or O^{2-} from their sites or by oxidation of Bi^{3+} into Bi^{5+} [14,15]. This defect structure results in various trapping centers with different depths since $Bi_4Ge_3O_{12}$ lattice structure contains several non-equivalent oxygen sites. Kovács *et al.*[16] have determined a thermoluminescent peak of $Bi_4Ge_3O_{12}$ at 130 °C, with activation energy of 0.86 eV, and all the other trap centers of BGO were detected at lower temperatures[17,18,19]. As the band gap of $Bi_4Ge_3O_{12}$ was determined to be 5.0 eV at room temperature[20], the activation energy E_a = (1.41 ± 0.04) eV observed in this work could be related to deeper traps than those registered by Kóvacs *et al.*[3z]. It can be hypothesized that the conduction mechanism in BGO is due to hopping electrons and that, at low frequencies, it is dominated by the electrons released from these deep traps.

3.2. Dielectric Characterization

In a dielectric under external oscillating field, the answer of the system can be expressed in terms of the complex dielectric permittivity ε*:

$$\varepsilon^*(\omega) = \varepsilon'(\omega) + i\varepsilon''(\omega) \quad (3)$$

which is obtained from the complex impedance data Z* by the expression[21]:

$$\varepsilon^* = \left(i\omega\varepsilon_0 \frac{S}{\ell} Z^* \right)^{-1} = \varepsilon' + i\varepsilon'' \quad (4)$$

where S is the electrode area, ℓ is the pellet thickness and ε_0 is the vacuum permittivity. The real part ε' is the relative permittivity, or dielectric constant, and the imaginary part ε'' is the loss factor.

The real and imaginary parts of complex permittivity of BGO were used to evaluate its dependence on frequency. Figure 6 shows log-log plots of ε' and ε'' at several temperatures. For frequency values higher than 10^3 Hz, ε' presented a weak dependency on the frequency or temperature. The dielectric constant, calculated from the average value over the frequency range of 10^3 to 10^6 Hz and several temperatures between 550 and 750 °C, was ε' = 20 ± 2. This value is consistent with the value ε' = 16 determined by Link *et al.*[6] at f = 10^3 Hz over the temperature range of 6 to 325 K.

No loss peak was observed in the ε'' spectra, characterizing a deviation from the dipolar response of the system, predicted by the Debye theory[22]. This feature indicates that the applied field interacts with the material not only through reorientation of the electric dipoles[9,10,23], but also through the displacement of the charge carriers, in accordance with the hopping-type conduction proposed for BGO in this work.

4. Conclusions

The electrical and dielectric properties of $Bi_4Ge_3O_{12}$ single crystals, in the frequency interval of 10^2 -10^6 Hz and temperature interval of 500 to 750 °C, were reported by the first time in the present work.

Impedance measurements of $Bi_4Ge_3O_{12}$ single crystals allowed us to determine an unique electrical process, identified by a single semicircle in the complex diagrams. The electrical conductivity curves agree with that proposed by

Dyre for conduction mechanisms over a random distribution of energy barriers in a disordered solid. Our results provided some evidence that the conduction process is associated to defects in the $(BiO_6)^{9-}$ octaedra. As these octaedra are deformed, they can give rise to trapping centers with different depths, which result in a distribution of energy barriers for the conduction process.

The real part of the complex dielectric permittivity was $\varepsilon' = 20 \pm 2$ for frequency values higher than 10^3 Hz for all the measured temperatures, and presented a low-frequency dispersion. This feature, combined to the absence of a loss peak in the ε'' *vs.* f curve, characterized a deviation from the dipolar response of the system. Both electrical and dielectric behaviors of BGO are typical of systems in which the charge-carrier polarization dominates the dielectric response.

Acknowledgments

The authors acknowledge CNPq, CAPES and FAPESP by the financial support.

References

1. Raymond, S.G.; Townsend, P.D. The influence of rare-earth ions on the low-temperature thermoluminescence of $Bi_4Ge_3O_{12}$, *J. Phys. Cond. Mat.,* v. 12, p. 2103-122, 2000.
2. Williams, P.A.; Rose, A.H.; Lee, K.S.; Conrad, D.C.; Day, G.W.; Hale, P.D. Optical, thermo-optic, electro-optic, and photoelastic properties of bismuth germanate ($Bi_4Ge_3O_{12}$), *Appl. Opt.,* v. 35, n. 19, p. 3562-69, 1996.
3. Macedo, Z.S.; Silva, R.S.; Valerio, M.E.G.; Martinez, A.L.; Hernandes, A.C. Laser Sintered Bismuth Germanate Ceramics as Scintillator Devices, accepted for publication in the *J. Am. Ceram. Soc*., 2003.
4. Nitsche, R. Crystal growth and electro-optic effect of bismuth germanate, $Bi_4(GeO_4)_3$, *J. Appl. Phys*. v. 36, p. 2358-60, 1965.
5. Li, C.; Yoshino, T. Simultaneous measurement of current and voltage by use of one bismuth germanate crystal, *Appl. Opt.,* v. 41, n. 25, p. 5391-97, 2002.
6. Link, J.; Fontanella, J. Temperature variation of the dielectric properties of bismuth germinate and bismuth germanium oxide", *J. Appl. Phys*., v. 51, n. 8, p. 4352-55,1980.
7. Jonhson, D. software Zview – v. 2, 3d, Scribner Associates, Inc., 2000.
8. Sinclair, D.C.; West, A.R. Electrical properties of a $LiTaO_3$ single crystal, Phys. Rev. B, v. 39, n. 18, p. 13486-13492, 1989.
9. Jonscher, A.K. The universal dielectric response, *Nature*, v. 267, p. 673-678, 1977.
10. Niklasson, G.A. Comparison of dielectric response functions for conducting materials, *J. Appl. Phys.*, v. 66, n. 9, p. 4350-59, 1989.
11. Bianchi, R.F.; Carrió, J.A.G.; Cuffini, S.L.; Mascarenhas Y.P.; Faria, R.M. Electrical conductivity of $SrTi_{1-x}RuxO_3$, *Phys. Rev. B,* v. 62, n. 6, p. 10785-89, 2000.
12. Dyre, J.C. The random free-energy barrier model for ac conduction in disordered solids, *J. Appl Phys.* v. 64. n. 5, p. 2456-68, 1988.
13. Smet, F.M. Crystal Growth and Characterization of Bismuth Germanate (BGO), PhD thesis, Katholieke Universiteit van Nijmegen, p. 113, 1989.
14. Lecoq, P.; Li, P.J.; Rostaing, B. BGO radiation damage effects: optical absorption, thermoluminescence and thermoconductivity, *Nucl. Instr. Meth. Phys. Res.*, v. A300, p. 240-258, 1991.
15. Raymond, S.G.; Luff, B.J.; Townsend, P.D.; Feng, S.; Hu, G. Thermoluminescence spectra of doped Bi4Ge3O12, *Radiat. Meas*., v. 23, n. 1, p. 195-202, 1994.
16. Kóvacs, L.; Raymond, S.G.; Luff, B.J.; Péter, A.; Townsend, P.D. Thermoluminescence spectra of eulytine $Bi_4Si_3O_{12}$ and $Bi_4Ge_3O_{12}$ single crystals, *Journal of Luminescence,* v. 60&61, p. 574-577, 1994.
17. Sabharwal, S.C.; Prasad, H.; Desai, D.G.; Sangeeta, H.P.; Karandikar, S.C.; Gupta, M.K. Thermoluminescence and transmission recovery of gamma irradiated $Bi_4Ge_3O_{12}$ single crystal, *Nucl. Instrum. Meth.,* v. A329, n. 1-2, p. 179-82, 1993.
18. Sangeeta, H.P.; Sabharwal, S.C. Crystal stoichiometry and thermoluminescence of $Bi_4Ge_3O_{12}$ and $Y_3Al_5O_{12}$, *J. Cryst. Growth*, v. 118, n. 3-4, p. 396-400, 1992.
19. Melcher, C.L. Correlation between thermoluminescence and radiation damage in bismuth germanate, *IEEE T. Nucl. Sci.*, v. 32,n. 1, p. 545-48, 1985.
20. Barnes, R.G.L. Bismuth Germanate (BGO) optimization for energy resolution and purity, IEEE Tans. Nucl. Sci., v. 31, n. 1, p. 249-252, 1984.
21. Macdonald, J.R. John Wiley & Sons, p. 12-43, 1987.
22. Elissalde, C.; Ravez, J. Ferroelectric ceramics: defects and dielectric relaxation, *J. Mat Chem.*, v. 11, n. 8, p. 1957-67, 2001.
23. Jonscher, A.K. Dielectric relaxation in solids, *J. Appl Phys.,* v. 32, p. R57-R70, 1999.